

Experimental Investigation of Drain Noise in High Electron Mobility Transistors: Thermal and Hot Electron Noise

Bekari Gabritchidze[®], Justin H. Chen[®], Kieran A. Cleary[®], Anthony C. Readhead[®], and Austin J. Minnich[®]

Abstract—We report the on-wafer characterization of S-parameters and microwave noise temperature (T_{50}) of discrete metamorphic InGaAs high electron mobility transistors (mHEMTs) at 40 and 300 K and over a range of drain-source voltages (V_{DS}). From these data, we extract a small-signal model (SSM) and the drain (output) noise current power spectral density (S_{id}) at each bias and temperature. This procedure enables S_{id} to be obtained while accounting for the variation of SSM, noise impedance match, and other parameters under the various conditions. We find that the noise associated with the channel conductance can only account for a portion of the measured output noise. Considering the variation of output noise with physical temperature and bias and prior studies of microwave noise in quantum wells, we hypothesize that a hot electron noise source (NS) based on real-space transfer (RST) of electrons from the channel to the barrier could account for the remaining portion of S_{id} . We suggest further studies to gain insights into the physical mechanisms. Finally, we calculate that the minimum HEMT noise temperature could be reduced by up to \sim 50% and \sim 30% at cryogenic temperature and room temperature, respectively, if the hot electron noise were suppressed.

Index Terms—Cryogenic electronics, drain noise, high electron mobility transistors, low-noise amplifiers, microwave noise, real-space transfer (RST).

I. INTRODUCTION

HIGH electron mobility transistors are widely employed in microwave amplifiers due to their low-noise characteristics [1], [2], [3], [4], [5]. While significant improvements

Manuscript received 12 July 2024; accepted 8 August 2024. Date of publication 11 September 2024; date of current version 24 September 2024. This work was supported by the National Science Foundation under Grant 1911220. The review of this article was arranged by Editor J. Mateos. (Corresponding author: Austin J. Minnich.)

Bekari Gabritchidze was with the Cahill Center for Astronomy and Astrophysics, Division of Physics, Mathematics and Astronomy, California Institute of Technology, Pasadena, CA 91125 USA. He is now with the Jet Propulsion Laboratory, Division of Physics, Mathematics and Astronomy, California Institute of Technology, Pasadena, CA 91125 USA (e-mail: bekarig@jpl.nasa.gov).

Justin H. Chen and Austin J. Minnich are with the Division of Engineering and Applied Science, California Institute of Technology, Pasadena, CA 91125 USA (e-mail: jchen10@caltech.edu; aminnich@caltech.edu).

Kieran A. Cleary and Anthony C. Readhead are with the Division of Physics, Mathematics and Astronomy, California Institute of Technology, Pasadena, CA 91125 USA (e-mail: kcleary@astro.caltech.edu; acr@astro.caltech.edu).

Color versions of one or more figures in this article are available at https://doi.org/10.1109/TED.2024.3445889.

Digital Object Identifier 10.1109/TED.2024.3445889

have been made in their noise performance in past decades [6], [7], [8], [9], [10], achieving further improvements requires a physics-based understanding of the origin of microwave noise which is lacking. Presently, noise in HEMTs is interpreted with the Pospieszalski model [11] in which noise is defined by two uncorrelated noise generators at the input (S_{vg}) and output (S_{id}) . The input noise generator, S_{vg} , is described using a noise temperature T_g which is assigned to the intrinsic gate resistance, and this noise temperature is generally interpreted as the physical temperature of the gate resistance [12], [13]. The gate resistance thermal noise is significantly larger than the induced gate noise for frequencies far below the cut-off frequency [14]. The output noise generator, S_{id} , is described by assigning a noise temperature, T_d , to the intrinsic output conductance g_{ds} . T_d is generally taken as a fitting parameter. Gate and drain noise are assumed to be uncorrelated at the analyzed frequencies. Despite the utility of the model in interpreting noise measurements on HEMTs, it is unable to provide insight into the physical origin of the output noise.

Other works have proposed various mechanisms; for instance, thermal noise has been suggested as the origin of channel noise in field effect transistors (FETs) [15] such as HEMTs [16], [17] and MOSFETs [18], [19]. A recent work attributed HEMT drain noise to suppressed shot noise [20] while others link it to a combination of thermal and suppressed shot noise [21].

Another theory attributes drain noise to microwave partition noise arising from real-space transfer (RST) [22], a process that has been investigated in early studies of transport and noise in quantum wells [23], [24], [25], [26], [27]. In this mechanism, electrons are heated out of equilibrium with the lattice by the electric field to physical temperatures exceeding 1000 K, a temperature sufficiently high that some electrons may thermionically emit out of the channel into the barrier. Because the barrier mobility is substantially less than that of the channel, two dissimilar conduction pathways exist from source to drain, creating partition noise [28] at the HEMT output. However, which of these mechanisms is the actual origin of drain noise in low-noise HEMTs remains under investigation.

In this article, we performed on-wafer S-parameter and microwave noise measurements (T_{50}) of discrete metamorphic InGaAs high electron mobility transistors (mHEMTs) at 40 and 300 K and various $V_{\rm DS}$ using a cryogenic probe

station (CPS). At each temperature and bias, we extracted a small-signal model (SSM) and noise parameters from the S-parameter and T_{50} measurements, allowing the output current noise power spectrum density (PSD), Sid, to be extracted while accounting for changes in small-signal parameters and optimal noise impedance at each condition. We find that the variation of S_{id} with physical temperature is inconsistent with suppressed shot noise as the sole noise source (NS), and further, that S_{id} cannot be explained only by noise associated with the channel conductance. Considering the findings of prior studies of microwave noise in quantum wells, we propose that the additional hot-electron noise is due to RST of electrons from the channel to the barrier, and we suggest how this hypothesis could be tested in future studies. Finally, we compute that the minimum noise temperature could be decreased by 50% and 30% at cryogenic and room temperature, respectively, if the hot-electron noise were suppressed.

This article is organized as follows. A description of the experimental setup and the modeling approach is presented in Section II. The measurements are presented in Section III. The contribution of channel diffusion noise to drain noise is examined in Section IV, followed by a discussion of the hot electron contribution to drain noise and a possible explanation based on RST in Section V. Finally, we provide a summary of the article in Section VI.

II. On-Wafer Cryogenic Characterization and Modeling

The S-parameters and the microwave noise temperature of metamorphic InGaAs mHEMTs (OMMIC, D007IH, 4F50, gate length $L_g=70$ nm, gate width W=0.2 mm) at various physical temperatures $T_{\rm ph}$ were measured using a CPS [29]. Details of the measurement procedure and the experimental set-up were described earlier [30]. The temperature of the sample stage was measured by a temperature sensor (Lakeshore DT670) and verified to vary by < 1 K over the sample stage. Thermal stability of the probes was verified by ensuring the bias tee temperature had equilibrated to a steady value after landing before any measurements were taken.

The S-parameter measurements were carried out in the frequency range 1–18 GHz using a vector network analyzer (VNA, Rhode&Schwartz ZVA50). The system was calibrated by transferring the measurement plane from the VNA to the tips of the wafer probes (GGB industries, 40A-GSG-100-DP) by through-reflect-match (TRM) and through-reflect-line (TRL) calibration on a CS-5 substrate. The two methods yielded SSM parameters that agreed to within 5% at 40 K. TRM was chosen in this work due to the reduced number of standards required for the calibration.

The microwave noise temperature was measured using the Y-factor method with a cold attenuator [30], [31] at a generator impedance of 50 Ω . The CPS was configured for noise measurements from 2 to 18 GHz. However, the measurement bandwidth was chosen from 5 to 15 GHz to minimize RF probe-pad contact time and avoid RF pad damage due to chuck vibrations arising from the closed loop He gas system. Because data at various frequencies are obtained by tuning a local oscillator frequency in our backend, for a given

bandwidth of 500 MHz, it takes more time to sample a wider frequency range. Therefore, limiting the bandwidth to 5–15 GHz decreased the time the probes need to be landed on the device.

Two 10 dB attenuators (Quantum Microwave), one at room temperature and one cryogenic, were inserted between the NS (Keysight, N4002A) and the device under test (DUT). The effective-noise ratio of the NS was calibrated by Keysight. The value was around 15 dB. The room-temperature attenuator was connected directly to the NS to reduce the change in output reflections from the "on" to "off" state of the NS, while the cryogenic attenuator was connected to the RF input probe contacting the input of the DUT and served as a cold load. The temperatures of the hot and cold powers presented to the DUT were 116 and 55 K, respectively.

A low noise amplifier (Cosmic Microwave, CIT1-18) was placed after the output probe and thermally strapped to the cold stage. A combination of mixer, oscillator, filters, amplifiers, and a power sensor was used outside the probe station to further process and measure the incident noise power. A detailed schematic was presented in [30]. The backend noise temperature was measured using a *Y*-factor method with the probes landed on a through and found to have a value of $\approx 100 \text{ K}$. We checked the calibration of the backend by landing the output probes on a 50 Ω load and measuring the power at two different temperatures by varying the chuck temperature. This approach gave a backend noise temperature which was within 1–2 K of the *Y* factor value.

An analysis indicated that the uncertainty in DUT noise temperature arose primarily from uncertainty in the input loss. These losses consist of stainless steel coaxial cable, cryogenic 10 dB attenuator, cryogenic bias tee, and the input RF probe. The losses of each component were characterized in a separate cryogenic dewar at each temperature for which noise measurements were performed. The input loss, excluding the two 10 dB attenuators, was around 3 dB. As a check of the accuracy of the individual loss measurements, we measured the insertion loss of the entire chain using S_{11} and S_{21} measurements on an open and through, respectively. The loss values were found to agree to within 0.1 dB. The insertion loss of the input RF probe was measured at room temperature by measuring the return loss with the probe tips open, but it could not be measured at cryogenic temperatures. Its temperature was assumed to be that of the cryogenic bias tee connected to the RF probe. Considering these uncertainties, a value of 0.1 dB uncertainty on the input loss was assumed. This uncertainty yields an absolute uncertainty in T_{50} of \approx 20% (\approx 15%) at 40 K (300 K). The repeatability of the T_{50} measurements was $\lesssim 0.5$ K (≈ 1 K) at 40 K (300 K).

From the *S*-parameter and T_{50} measurements, a SSM and noise model of the device were developed. Several models of varying complexity have been reported for HEMTs [33], [34], [35], [36], [37]. Since our focus is on the physical mechanism of output noise, we use a relatively simple 15-element SSM shown in Fig. 1 as originally described in [32]. This model allows decomposition of the measured noise into input and output generators. We followed an equation-based approach for extraction following that given in [38, pp. 257–259].

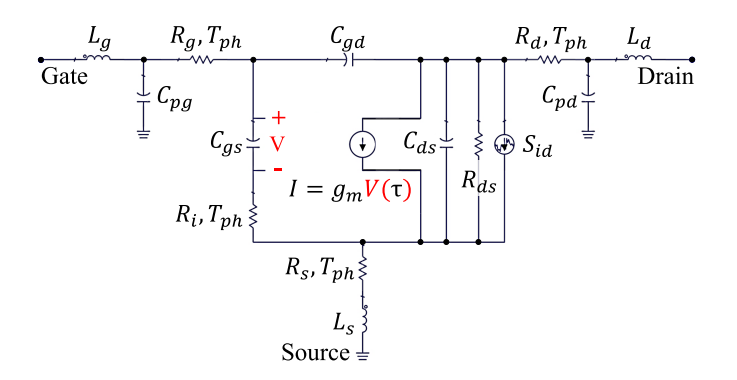


Fig. 1. SSM used to extract intrinsic small-signal properties and noise model of the device following that given in [32]. The temperatures of the noise generators associated with parasitic resistances are also specified. Drain noise is described by an output current noise generator, S_{id} .

In brief, we measured the S-parameters, from which Y-parameters were computed and the parasitic capacitances removed. Z-parameters were then computed to allow for removal of L_g and R_g (gate inductance and resistance), and then converted to Y-parameters to directly calculate the first estimate of intrinsic parameters. Simulated annealing and quasi-Newton optimization, available in advanced design system (ADS, Keysight), were then used to minimize a least-square error function following [30]. After the optimization, the intrinsic parameters were further fine-tuned to improve the agreement between the measured and simulated S-parameters.

Temperature independence of the extracted parasitic capacitances and inductances was assumed based on [39] and [40], and the 300 K values were used at all $T_{\rm ph}$. The parasitic resistances (R_g, R_s, R_d) have been reported to vary $\approx 50\%$ as $T_{\rm ph}$ is decreased from 300 to 40 K [40]; however, measuring these resistances require either wider band measurements or special test structures which were not available. To constrain the impact of this assumption, we estimated the effect of decreasing parasitic resistances by 50% in the 40 K SSM on the SSM parameters and S_{id} . We found that this change altered g_m and $R_{\rm ds}$ by $\approx 5\%$ and $S_{\rm id}$ by $\approx 6\%$. Therefore, we neglected the temperature-dependence of the parasitic resistances. Additionally, the parasitics are bias-independent [40], so at a given $T_{\rm ph}$, the observed $V_{\rm DS}$ -dependent trends are not affected by the assumption of constant parasitic resistance. However, the absolute values of minimum noise temperature (T_{\min}) with V_{DS} at $T_{\rm ph} = 40$ K are overestimated by $\approx 10\%$ at 6 GHz when the parasitic resistance at 300 K is used for all temperatures. SSM parameter extraction could be carried only for $V_{DS} \ge 0.1 \text{ V}$, as the SSM requires the device to exhibit at least 10 dB of gain to fit the experimental data to within $\approx 2\%$.

Under these assumptions, a noise model based on the Pospieszalski model [11] was obtained by fitting the measured and modeled T_{50} using $S_{\rm id}$ as a fitting parameter. The uncertainties in $S_{\rm id}$ reported as the error bars in the subsequent figures include the uncertainties in access resistances, $g_{\rm ds}$ and T_{50} measurements; however, the total uncertainty in $S_{\rm id}$ is dominated by the uncertainty in our T_{50} measurements.

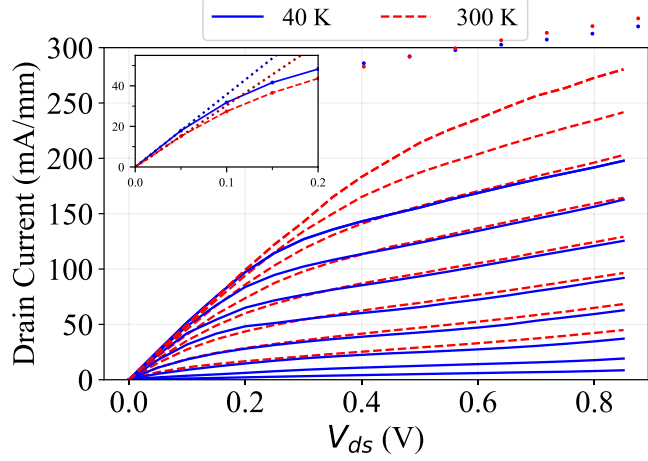


Fig. 2. Measured $I_{\rm DS}-V_{\rm DS}$ characteristics at 40 K (blue) and 300 K (red) for various $V_{\rm GS}$ ranging from -0.3 to -0.02 V in steps of 0.06 V. Inset: magnified view of the origin for $V_{\rm GS}$ set to -140 mV (-220 mV) at 40 K (300 K), along with linear fits.

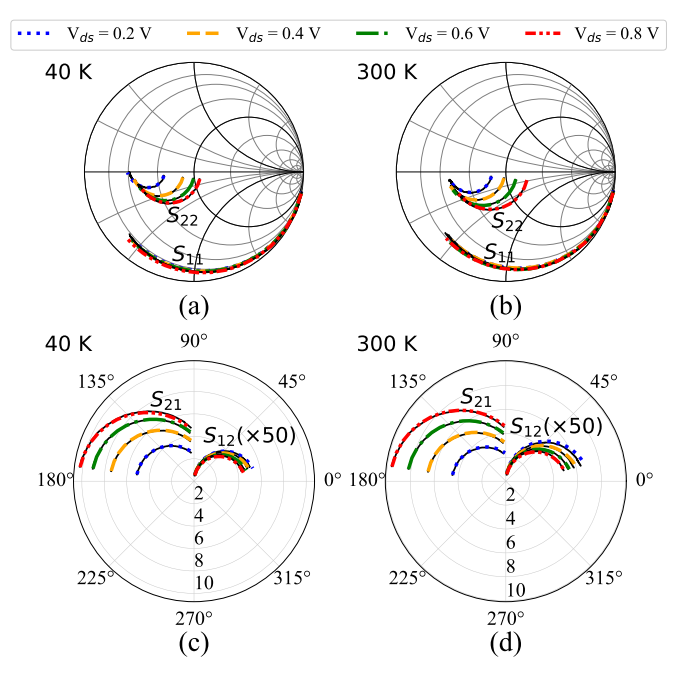


Fig. 3. Measured S_{11} and S_{22} in a Smith chart at (a) 40 K and (b) 300 K, and S_{12} and S_{21} in a polar plot at (c) 40 K and (d) 300 K. S_{12} has been multiplied by 50 to facilitate plotting. Frequency varies over 1 – 18 GHz. The measurements at various $V_{\rm DS}$ are shown (broken colored lines). The modeled S parameters are also shown (black solid lines). $V_{\rm GS}$ was held constant for all $V_{\rm DS}$ with $V_{\rm GS}=-136$ mV (-226 mV) at 40 K (300 K).

III. RESULTS

Fig. 2 shows the measured $I_{\rm DS}-V_{\rm DS}$ characteristics at 40 and 300 K at various $V_{\rm GS}$. The measurements are in good qualitative agreement with measurements on other HEMTs [6]. Fig. 3 shows the measured and modeled S-parameters at various $V_{\rm DS}$ ranging from 0.2 to 0.8 V and physical temperatures of 40 and 300 K. At a given $T_{\rm ph}$, S_{21} and S_{22} exhibit the largest variation with $V_{\rm DS}$, while S_{12} and S_{11} show smaller but observable dependence.

These measurements were used as input to the extraction procedure described in Section II. Representative SSM

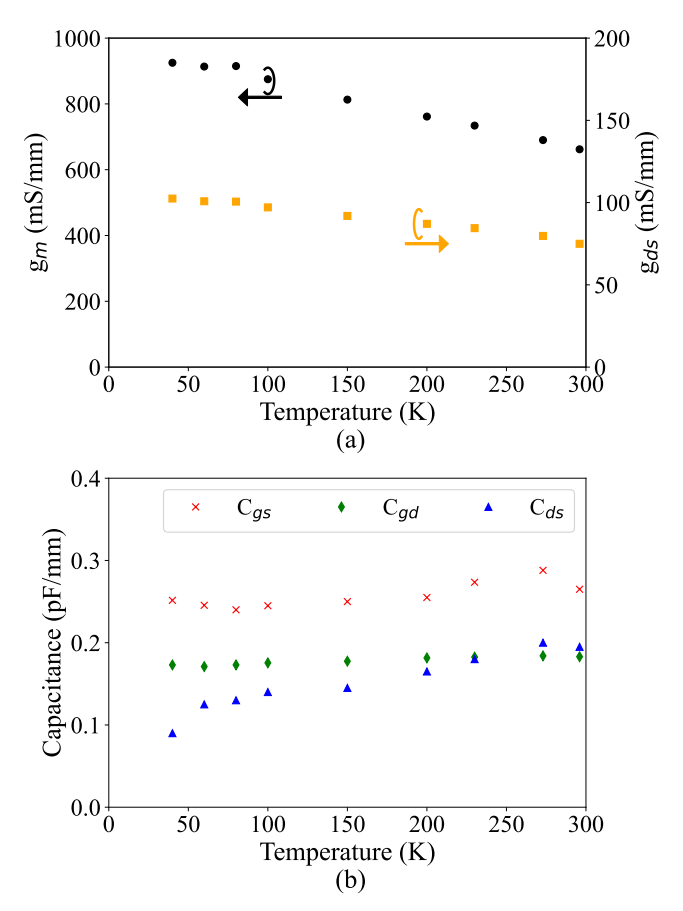


Fig. 4. Extracted (a) g_m and g_{ds} and (b) small-signal capacitances versus temperature at $V_{\rm DS}=0.6$ V and $I_{\rm DS}=10$ mA (50 mA/mm).

parameters such as g_m and g_{ds} [Fig. 4(a)] and various capacitances [Fig. 4(b)] are shown versus temperature at $V_{DS} = 0.6 \text{ V}$ and $I_{DS} = 10 \text{ mA}$ (50 mA/mm). The values and trends with temperature are in good qualitative agreement with other reports on low-noise HEMTs [39].

In Fig. 5, the measured T_{50} versus frequency is shown for various $V_{\rm DS}$ and the two physical temperatures. In both the S-parameter and noise measurements, the gate voltage ($V_{\rm GS}$) was kept constant at $V_{\rm GS} = -136$ mV (-226 mV) at 40 K (300 K), for all $V_{\rm DS}$. These $V_{\rm GS}$ were selected so that $I_{\rm DS} = 20$ mA (100 mA/mm) at $V_{\rm DS} = 0.8$ V and a given $T_{\rm ph}$. At a given $V_{\rm GS}$ and $T_{\rm ph}$, the threshold voltage ($V_{\rm th}$) varied with $V_{\rm DS}$ from -0.23 to -0.28 V at 40 K and -0.31 to -0.38 V at 300 K. The $V_{\rm th}$ at each temperature was calculated from the $I_{\rm DS}$ - $V_{\rm GS}$ curves following [41]. $V_{\rm DS}$ was varied from 0.1 to 1.0 V; $V_{\rm DS}$ was restricted to ≤ 1.0 V so that gate leakage currents ($I_{\rm G}$) were $I_{\rm G} \lesssim 20$ μ A/mm at $T_{\rm ph} = 300$ K, leading to negligible contribution from shot noise [42].

The lowest $T_{\rm ph}$ was limited to 40 K to avoid cryogenic self-heating effects in which the dissipated power from the external bias leads to the device temperature exceeding the cryostat temperature. Previous studies have found that this effect is negligible in GaAs or InP HEMTs for $T_{\rm ph} > 40$ K for typical low-noise biases [43], [44], [45] (c.f. [45, Fig. 4(a)] which shows that gate temperature and physical temperature coincide above around 20 K).

From these measurements, a noise model was developed which permits the extraction of S_{id} of the intrinsic device

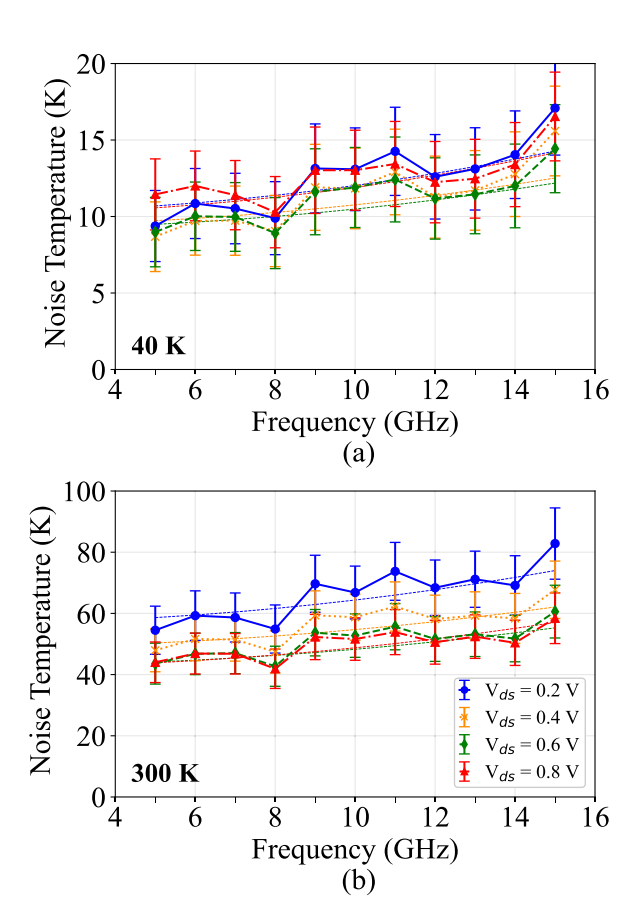


Fig. 5. Measured T_{50} versus frequency (symbols) at various $V_{\rm DS}$ and physical temperature of (a) 40 K and (b) 300 K. The fit of the noise model is also shown (dashed lines). $V_{\rm GS}$ remained constant at all $V_{\rm DS}$ with $V_{\rm GS}=-136$ mV and $V_{\rm GS}=-226$ mV at 40 and 300 K, respectively. These $V_{\rm GS}$ were selected so that $I_{\rm DS}=20$ mA (100 mA/mm) at $V_{\rm DS}=0.8$ V and a given $T_{\rm Dh}$.

at each bias and temperature using the measured T_{50} and S-parameters while accounting for mismatch between 50 Ω and optimum noise impedance. Following the CMOS and MOSFET noise literature [46], [47], [48], [49], we plot $S_{\rm id}$ versus $V_{\rm DS}$ at 40 and 300 K in Fig. 6(a) and (b), respectively. At 40 K, $S_{\rm id}$ follows a linear trend at low $V_{\rm DS} \lesssim 0.6$ V and rises rapidly at higher voltages. A similar trend is found at 300 K.

We note that it is expected that as $V_{\rm DS}$ tends to zero, $S_{\rm id}$ should equal the value from the Johnson-Nyquist expression [corresponding to $\gamma \to 1$ in (1)] indicated as the dashed red lines in Fig. 6. [50, Fig. 2] However, the measured values of S_{id} are still larger than the Johnson-Nyquist value at $V_{\rm DS} = 0.1$ V, the lowest value for which we can accurately extract a noise model. We attribute this discrepancy to the fact that even at $V_{\rm DS} = 0.1$ V, the electric field under the gate is estimated conservatively as 0.1 V/ $L_g \approx 10$ kV/cm, which is in the high-field regime. This estimation is supported by the I-V characteristics in the inset of Fig. 2, which show that the measured characteristics for the V_{GS} used in Fig. 6 deviate from the linear trend even at 0.1 V, indicating that the device is entering saturation at this bias. Thus, observation of the limit of Johnson-Nyquist noise is not expected in the bias range considered here.

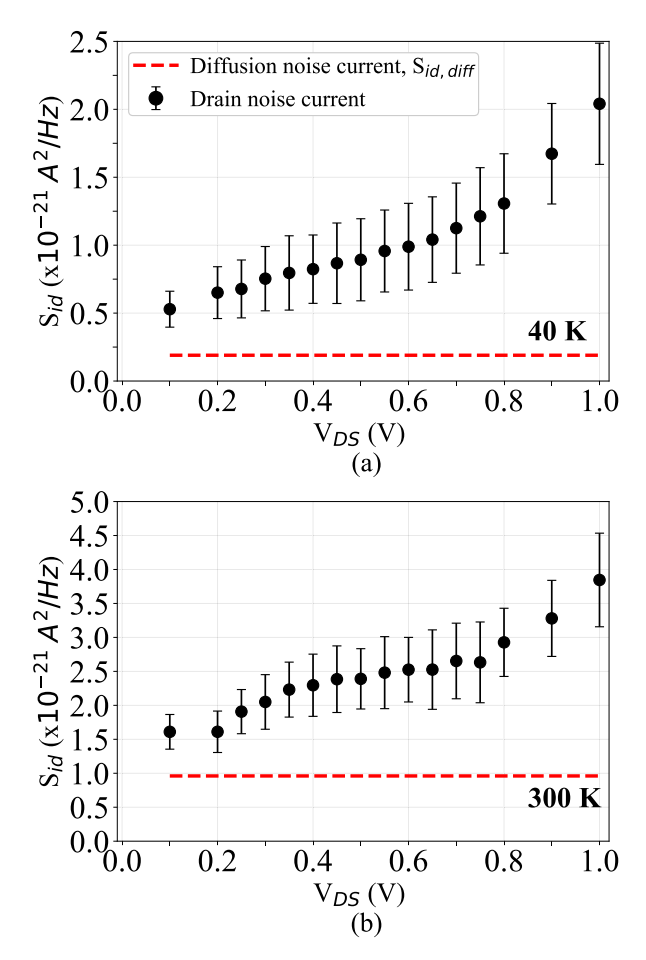


Fig. 6. Extracted S_{id} (black circles) and predicted channel diffusion noise PSD $S_{id,\text{diff}}$ (red dashed line, $\gamma=1$) versus V_{DS} at (a) 40 K and (b) 300 K. The measured S_{id} is inconsistent with channel diffusion noise as the sole NS. The gate voltage, V_{GS} was -136 mV (-226 mV) at 40 K (300 K), yielding $I_{\text{dS}}=20$ mA (100 mA/mm) at $V_{\text{DS}}=0.8$ V. These gate voltages were selected to ensure adequate gain at low V_{DS} for extraction.

Regarding the rapid increase in $S_{\rm id}$ at high voltages, we note that no indications of nonideal effects like impact ionization were present in the dc characteristics or S-parameters in our devices. The I-V curves (Fig. 2) did not exhibit any kinks, while the gate–source current, $I_{\rm GS}$, remained at values between -5 and $-20~\mu{\rm A/mm}$, far from the bias regime where impact ionization was observed previously in these devices [51, Fig. 6.7]. Additionally, S_{22} remained capacitive for all $V_{\rm DS}$ [52]. However, it has been reported based on Monte Carlo simulations [53] that microwave noise from impact ionization may occur even though it may not be observable in I-V and S-parameter measurements. Therefore, it is possible that the rapid increase in $S_{\rm id}$ above 0.8 V is due to impact ionization.

The variation of T_d with $T_{\rm ph}$ for the present devices has been previously reported in [30]. Here, we present $S_{\rm id}$ versus $T_{\rm ph}$ at constant $V_{\rm DS}=0.6$ V and $I_{\rm DS}=10$ mA (50 mA/mm) in Fig. 7. A dependence of $S_{\rm id}$ on $T_{\rm ph}$ is observed. This observation contradicts the predictions of suppressed shot noise theory. According to this theory, if $I_{\rm DS}$ is kept constant with physical temperature, then the output noise current $S_{\rm id}$ is predicted to be temperature-independent [20], [54], [55]. This prediction is inconsistent with the measured temperature dependence of the

output noise current in Fig. 7. This conclusion agrees with the findings of [30], [39], [56], and [57]. This finding indicates that suppressed shot noise cannot be the sole mechanism contributing to drain noise.

IV. CONTRIBUTION OF CHANNEL DIFFUSION NOISE TO OUTPUT NOISE

We now discuss what physical mechanisms could account for the observed trends of drain noise PSD. Drain noise in HEMTs, like other FETs, is expected to originate at least in part from thermal noise of the channel conductance. Away from equilibrium, this noise is referred to as "diffusion noise" owing to the relation between PSD and diffusion coefficient [25]. The relevant portion of the channel of interest for its noise contribution is that under the gate recess, as the other access resistances have been already taken into account in the SSM. The diffusion noise of the channel subject to gate and drain biases is given by

$$S_{\rm id,diff} = 4k_B g_{\rm dso} T_{\rm ph} \gamma \tag{1}$$

where k_B is the Boltzmann's constant, g_{dso} is the channel conductance at $V_{\rm DS}=0$ V, and γ is a factor that accounts for the variation in carrier density along the channel due to the combined effect of the gate-source and drain-source potentials [16], [47], [49]. At equilibrium and in the linear region, $\gamma = 1$, while in saturation, its values depend on the channel length; in the long-channel limit $\gamma = 2/3$ using the gradual-channel approximation, while in short-channel devices, γ varies between 1 and 2 due to short-channel effects such as velocity saturation and channel-length modulation [47], [58], [59]. $S_{id,diff}$ is also affected by high-field effects such as nonequilibrium carrier heating, meaning that electrons are heated above the lattice temperature. Although the higher electron temperature increases $S_{\rm id,diff}$, the high-field conductance is generally lower than the low-field value due to the decrease in mobility with increasing field. In addition, the carrier density in the pinch-off region is at least an order of magnitude lower than that of the unperturbed channel, [5] further lowering $S_{id,diff}$.

Considering these competing trends, various studies have concluded that the noise from the pinch-off region is negligible [47], [60], [61]. This conclusion is compatible with experimental measurements of microwave noise in InGaAs quantum wells, which show that the current PSD decreases with increasing field [25, Fig. 16.7]. Therefore, an overestimate for the channel diffusion noise may be obtained by taking $\gamma = 1$ in (1) and thereby neglecting the decrease in noise associated with the formation of the pinch-off region at high $V_{\rm DS}$. $g_{\rm dso}$ is obtained from the slope of the I-V characteristics at $V_{\rm DS} = 0$ V.

In Fig. 6(a) and (b), $S_{\rm id,diff}$ is shown at 40 and 300 K, respectively. The measured $S_{\rm id}$ exceeds $S_{\rm id,diff}$, corresponding to $\gamma = S_{\rm id}/S_{\rm id,diff} \approx 3$ –6 at 40 K and ≈ 2 –3 at 300 K. However, theories of channel diffusion noise including short-channel effects generally predict $\gamma \lesssim 1.5$ [47], [58]. Fig. 7 shows the temperature dependence of $S_{\rm id}$ and $S_{\rm id,diff}$ at constant $V_{\rm DS} = 0.6$ V and $I_{\rm DS} = 10$ mA (50 mA/mm). For the calculation of $S_{\rm id,diff}$, $g_{\rm dso}$ was obtained from the I-V curves at

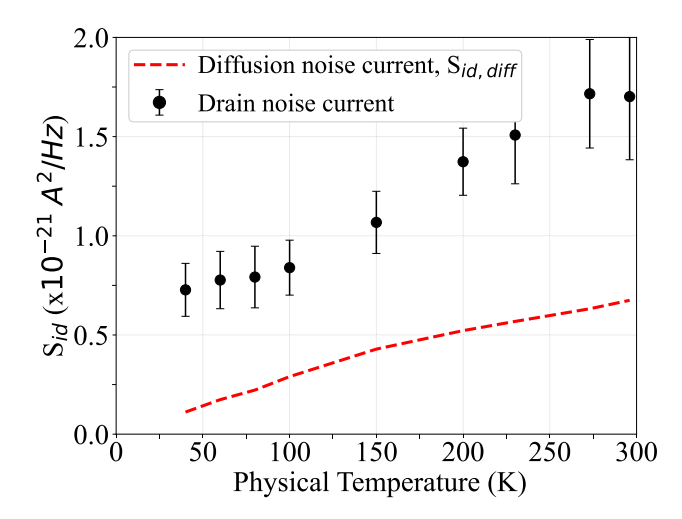


Fig. 7. Extracted S_{id} (black circles) versus physical temperature $T_{\rm ph}$ and predicted $S_{id,\rm diff}$ (red dashed line, $\gamma=1$) at constant $V_{\rm DS}=0.6$ V and $I_{\rm DS}=10$ mA (50 mA/mm), a typical low-noise bias.

each temperature and was corrected for the access resistances following [49], [62]. While $S_{\rm id,diff}$ qualitatively accounts for the temperature-dependence of $S_{\rm id}$, the measured trend plateaus below 100 K while $S_{\rm id,diff}$ tends to zero with decreasing temperature. Additionally, the magnitude of $S_{\rm id,diff}$ is $\approx 50\%-70\%$ lower than the measured values. Considering the totality of the observations, the analysis suggests that another mechanism beyond channel diffusion noise contributes to drain noise in HEMTs.

V. DISCUSSION

We now discuss potential physical origins of the additional drain NS. Suppressed shot noise can arise if electrons propagate quasi-ballistically in the channel. However, ultrafast optical studies have found that photoexcited electrons in quantum wells thermalize within 200 fs, implying an electron–electron collision time on the order of 10 fs [63, Sec. 4C3b]. Considering a drift velocity of $\approx 5 \times 10^7$ cm s⁻¹ [64], these values yield a mean free path of around 5–10 nm. This value is much shorter the gate length or source–drain separation of even highly scaled HEMTs, implying that suppressed shot noise is not likely to be a relevant noise mechanism in HEMTs.

Another theory for drain noise based on RST of hot electrons from the channel to barrier films was developed following the conclusions of prior studies of microwave noise in quantum wells [22]. Specifically, in earlier experimental works, the microwave noise temperature was found to be affected by alterations to the quantum well potential even with the channel alloy composition held constant, suggesting that the heterojunction potential confining the channel electrons played a role in the noise mechanism [26], [27]. This observation is compatible with the RST mechanism in which hot electrons thermionically emit over the confining barrier potential to create partition noise. Esho et al. [22] derived an expression for $S_{\rm id}$ in which noise arises due to RST; however, this work did not consider the contribution of channel diffusion noise.

Here, we suggest that drain noise could be attributed to a combination of channel diffusion noise and RST: $S_{id} = S_{id,diff} + S_{RST}$. The S_{RST} is given by [22]

$$S_{\text{RST}} = S_{\text{RST},0} \exp(-(\Delta E_c - q V_{\text{ov}})/k_B T_e)$$
 (2)

where $S_{\rm RST,0}$ is a constant prefactor and q is the electric charge. The RST noise depends exponentially on the peak electron temperature, T_e , the conduction band discontinuity (ΔE_c) at the channel/barrier heterojunction, and the overdrive voltage defined as $V_{\rm ov} = V_{\rm gs} - V_{\rm th}$, where $V_{\rm th}$ is the threshold voltage. In [22], the peak electron temperature was assumed to vary linearly with the physical temperature. However, Monte Carlo studies [65] and the weak temperature-dependence of high-field velocity characteristics in many semiconductors indicate that the peak electron temperature in HEMTs should exhibit a weak dependence on lattice temperature. In this case, RST noise would be predicted to exhibit only a weak dependence on physical temperature as well. This conclusion differs from that originally reported in [22].

Qualitatively, the trend of S_{id} versus T_{ph} in Fig. 7 can be explained if the diffusion noise is responsible for the primary dependence of S_{id} on T_{ph} , with another mechanism with weaker temperature dependence accounting for the overall trend and magnitude. Using the numerical values given in [22] and assuming $V_{ov} = 43$ mV from the measurements in this work, we compute $S_{RST} \approx 0.3 \times 10^{-21}$ A²/Hz over the range of temperatures studied, which is of the right order of magnitude to explain the discrepancy. However, we caution that this estimate is only valid to within a factor of 2–3, owing to uncertainties in the parameters described in [22].

The role of RST in drain noise could be further confirmed by examining how the microwave noise temperature trends with bias and temperature are affected by changes in quantum confinement of channel electrons while keeping the channel composition fixed so as to avoid confounding effects from impact ionization. This modification can be accomplished by increasing the Al composition of the barrier [66]. Strained-barrier HEMTs with Al composition of over 55% have been reported [67], and so such a study appears feasible.

Finally, we use our noise model to estimate the magnitude of improvement in minimum noise temperature, T_{\min} , if the channel noise were only due to thermal noise. T_{\min} is the minimum possible noise temperature of the device with the optimal input impedance [68]. In Fig. 8, we plot the extracted T_{\min} , obtained from the noise model using S-parameter and T_{50} data versus $V_{\rm DS}$ at 40 and 300 K, and frequency of 6 GHz. In this plot, we also show the predicted trend of T_{\min} if drain noise was due solely to channel diffusion noise. We observe that the minimum T_{\min} could be improved by $\approx 50\%$ and $\approx 30\%$ at 40 and 300 K, respectively.

This result implies that if the hot-electron noise observed in $S_{\rm id}$ originates from RST, then significant improvements in cryogenic and room temperature noise performance may be possible by engineering the quantum well for improved quantum confinement. If such gains were realized, there are significant implications for the design and performance of large telescope arrays for radio astronomy, such as the planned 2000-dish Deep Synoptic Array (DSA-2000; [69]).

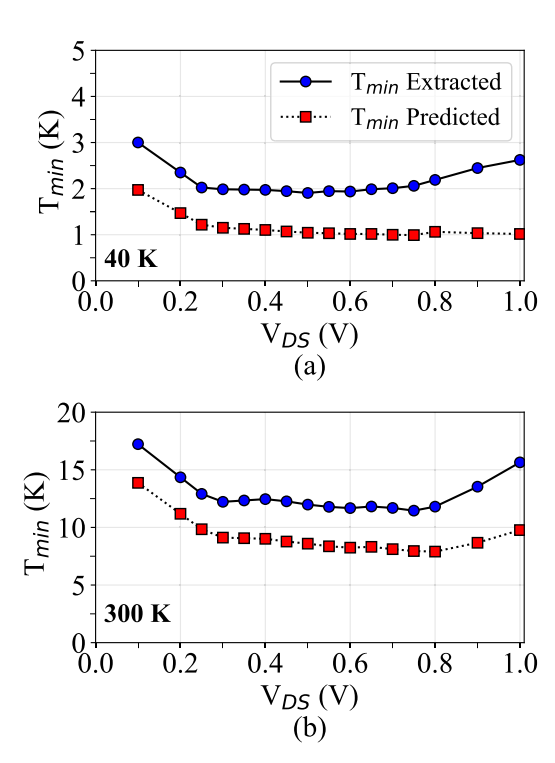


Fig. 8. Extracted $T_{\rm min}$ [30] and predicted $T_{\rm min}$ with only channel diffusion noise versus $V_{\rm DS}$ at (a) 40 K and (b) 300 K and constant $V_{\rm GS}=-136$ mV and $V_{\rm GS}=-226$ mV, respectively. The predicted $T_{\rm min}$ is obtained by setting $S_{id}=S_{id,\rm diff}$ in the noise model. All the above data are at 6 GHz. The $V_{\rm GS}$ in (a) and (b) were selected so that at both physical temperatures, $V_{\rm DS}=0.8$ V and $I_{\rm ds}=20$ mA (100 mA/mm).

A reduction in LNA noise temperature by 30% for the DSA-2000 would have the effect of increasing its survey speed by around 40%, representing a major increase in performance achieved by the cost-effective route of replacing the low-noise amplifier.

VI. CONCLUSION

We have characterized the *S*-parameters and the microwave noise temperature of InGaAs mHEMTs at various temperatures and biases. The extracted drain noise is found to exceed that expected from channel diffusion noise by a factor of ≈2–6, suggesting that an additional mechanism contributes to drain noise. Based on prior studies of microwave noise in quantum wells, we hypothesize that this noise mechanism is RST noise. We suggest approaches to further test this hypothesis. Finally, we estimate that improvements in minimum cryogenic noise temperature of up to 50% can be achieved if the hot-electron noise is suppressed.

ACKNOWLEDGMENT

The authors thank Jan Grahn, Pekka Kangaslahti, Jacob Kooi, Junjie Li, Jun Shi, and Sander Weinreb for useful discussions. The work described in this article was conducted while Bekari Gabritchidze was at the Cahill Center for Astronomy and Astrophysics, Division of Physics, Mathematics and Astronomy, California Institute of Technology, Pasadena, CA, USA.

REFERENCES

- [1] T. Mimura, "The early history of the high electron mobility transistor (HEMT)," *IEEE Trans. Microw. Theory Techn.*, vol. 50, no. 3, pp. 780–782, Mar. 2002.
- [2] P. E. Longhi, L. Pace, S. Colangeli, W. Ciccognani, and E. Limiti, "Technologies, design, and applications of low-noise amplifiers at millimetre-wave: State-of-the-art and perspectives," *Electronics*, vol. 8, no. 11, p. 1222, Oct. 2019.
- [3] A. Reinhard, "Ultra-low noise InP HEMTs for cryogenic applications— Fabrication, modeling and characterization," Ph.D. thesis, Dept. Inf. Technol. Elect. Eng., ETH Zurich, Zürich, Switzerland, 2013.
- [4] E. W. Bryerton, M. Morgan, and M. W. Pospieszalski, "Ultra low noise cryogenic amplifiers for radio astronomy," in *Proc. IEEE Radio Wireless Symp.*, Jan. 2013, pp. 358–360.
- [5] F. Schwierz and J. J. Liou, Modern Microwave Transistors: Theory, Design, and Performance, 1st ed., Hoboken, NJ, USA: Wiley, 2002.
- [6] E. Cha, N. Wadefalk, G. Moschetti, A. Pourkabirian, J. Stenarson, and J. Grahn, "A 300-μW cryogenic HEMT LNA for quantum computing," in *IEEE MTT-S Int. Microw. Symp. Dig.*, Aug. 2020, pp. 1299–1302.
- [7] E. Cha et al., "0.3-14 and 16-28 GHz wide-bandwidth cryogenic MMIC low-noise amplifiers," *IEEE Trans. Microw. Theory Techn.*, vol. 66, no. 11, pp. 4860–4869, Jan. 2018.
- [8] William. R. Deal et al., "Low noise amplification at 0.67 THz using 30 nm InP HEMTs," *IEEE Microw. Wireless Compon. Lett.*, vol. 21, no. 7, pp. 368–370, Jul. 2011.
- [9] F. Thome, F. Schäfer, S. Türk, P. Yagoubov, and A. Leuther, "A 67–116-GHz cryogenic low-noise amplifier in a 50-nm InGaAs metamorphic HEMT technology," *IEEE Microw. Wireless Compon. Lett.*, vol. 32, no. 5, pp. 430–433, May 2022.
- [10] D. Cuadrado-Calle et al., "Broadband MMIC LNAs for ALMA band 2+3 with noise temperature below 28 k," *IEEE Trans. Microw. Theory Techn.*, vol. 65, no. 5, pp. 1589–1597, May 2017.
- [11] M. W. Pospieszalski, "Modeling of noise parameters of MESFETs and MODFETs and their frequency and temperature dependence," *IEEE Trans. Microw. Theory Techn.*, vol. 37, no. 9, pp. 1340–1350, Oct. 1989.
- [12] M. W. Pospieszalski, "On the dependence of FET noise model parameters on ambient temperature," in *Proc. IEEE Radio Wireless Symp.* (RWS), Jan. 2017, pp. 159–161.
- [13] M. W. Pospieszalski, "Interpreting transistor noise," *IEEE Microw. Mag.*, vol. 11, no. 6, pp. 61–69, Oct. 2010.
- [14] P. Heymann and M. Rudolph, A Guide to Noise in Microwave Circuits: Devices, Circuits and Measurement, 1st ed., Hoboken, NJ, USA: Wiley, 2021
- [15] A. V. Der Ziel, "Thermal noise in field-effect transistors," *Proc. IRE*, vol. 50, no. 8, pp. 1808–1812, 1962.
- [16] A. van der Ziel and E. N. Wu, "Thermal noise in high electron mobility transistors," *Solid-State Electron.*, vol. 26, no. 5, pp. 383–384, May 1983.
- [17] A. van der Ziel, "Thermal noise in the hot electron regime in FET's," *IEEE Trans. Electron Devices*, vol. ED-18, no. 10, p. 977, Oct. 1971.
- [18] J. C. J. Paasschens, A. J. Scholten, and R. van Langevelde, "Generalizations of the Klaassen-Prins equation for calculating the noise of semiconductor devices," *IEEE Trans. Electron Devices*, vol. 52, no. 11, pp. 2463–2472, Nov. 2005.
- [19] A. S. Roy, C. C. Enz, and J.-M. Sallese, "Noise modeling methodologies in the presence of mobility degradation and their equivalence," *IEEE Trans. Electron Devices*, vol. 53, no. 2, pp. 348–355, Feb. 2006.
- [20] M. W. Pospieszalski, "On the limits of noise performance of field effect transistors," in *IEEE MTT-S Int. Microw. Symp. Dig.*, Jun. 2017, pp. 1953–1956.
- [21] K. Ohmori and S. Amakawa, "Direct white noise characterization of short-channel MOSFETs," *IEEE Trans. Electron Devices*, vol. 68, no. 4, pp. 1478–1482, Apr. 2021.
- [22] I. Esho, A. Y. Choi, and A. J. Minnich, "Theory of drain noise in high electron mobility transistors based on real-space transfer," *J. Appl. Phys.*, vol. 131, no. 8, Feb. 2022, Art. no. 085111.
- [23] A. Matulionis, V. Aninkevičius, J. Berntgen, D. Gasquet, J. Liberis, and I. Matulionien, "QW-shape-dependent hot-electron velocity fluctuations in InGaAs-based heterostructures," *Phys. Status Solidi B*, vol. 204, no. 1, pp. 453–455, Nov. 1997.
- [24] A. Matulionis, V. Aninkevičius, and J. Liberis, "Hot-electron velocity fluctuations in two-dimensional electron gas channels," *Microelectron. Rel.*, vol. 40, no. 11, pp. 1803–1814, Nov. 2000.
- [25] H. Hartnagel, R. Katilius, and A. Matulionis, Microwave Noise in Semiconductor Devices, 1st ed., Hoboken, NJ, USA: Wiley, 2001.

- [26] V. Aninkevicius et al., "Hot-electron noise and diffusion in AlGaAs/GaAs," Semiconductor Sci. Technol., vol. 9, no. 5S, pp. 576–579, May 1994.
- [27] V. Aninkevičius, V. Bareikis, J. Liberis, A. Matulionis, and P. Sakalas, "Comparative analysis of microwave noise in GaAs and AlGaAs/GaAs channels," *Solid-State Electron.*, vol. 36, no. 9, pp. 1339–1343, Sep. 1993.
- [28] A. Ambrozy, Electronic Noise. New York, NY, USA: McGraw-Hill, 1983.
- [29] D. Russell, K. Cleary, and R. Reeves, "Cryogenic probe station for onwafer characterization of electrical devices," *Rev. Sci. Instrum.*, vol. 83, no. 4, Apr. 2012, Art. no. 044703.
- [30] B. Gabritchidze, K. Cleary, J. Kooi, I. Esho, A. C. Readhead, and A. J. Minnich, "Experimental characterization of temperature-dependent microwave noise of discrete HEMTs: Drain noise and real-space transfer," in *IEEE MTT-S Int. Microw. Symp. Dig.*, Jun. 2022, pp. 615–618.
- [31] J. Fernandez, "A noise temperature measurement system using a cryogenic attenuator," TMO Prog. Rep., vol. 42, p. 135, Nov. 1998.
- [32] G. Dambrine, A. Cappy, F. Heliodore, and E. Playez, "A new method for determining the FET small-signal equivalent circuit," *IEEE Trans. Microw. Theory Techn.*, vol. 36, no. 7, pp. 1151–1159, Jul. 1988.
- [33] S. Khandelwal, Advanced SPICE Model for GaN HEMTs (ASM-HEMT): A New Industry-Standard Compact Model for GaN-based Power and RF Circuit Design. Cham, Switzerland: Springer, 2022.
- [34] F. Jazaeri and J.-M. Sallese, "Charge-based EPFL HEMT model," *IEEE Trans. Electron Devices*, vol. 66, no. 3, pp. 1218–1229, Mar. 2019.
- [35] U. Radhakrishna, T. Imada, T. Palacios, and D. Antoniadis, "MIT virtual source GaNFET-high voltage (MVSG-HV) model: A physics based compact model for HV-GaN HEMTs," *Phys. Status Solidi C*, vol. 11, nos. 3–4, pp. 848–852, Mar. 2014.
- [36] U. Radhakrishna, "A compact transport and charge model for GaN-based high electron mobility transistors for RF applications," M.S. thesis, Dept. Eng. Comput. Sci., Massachusetts Inst. Technol., Cambridge, MA, USA, Jun. 2013.
- [37] F. Jazaeri, M. Shalchian, and J.-M. Sallese, "Transcapacitances in EPFL HEMT model," *IEEE Trans. Electron Devices*, vol. 67, no. 2, pp. 758–762, Feb. 2020.
- [38] G. Kompa, *Parameter Extraction Complex Nonlinear Models*. Norwood MA, USA: Artech House, 2020.
- [39] F. Heinz, F. Thome, D. Schwantuschke, A. Leuther, and O. Ambacher, "A scalable small-signal and noise model for high-electron-mobility transistors working down to cryogenic temperatures," *IEEE Trans. Microw. Theory Techn.*, vol. 70, no. 2, pp. 1097–1110, Feb. 2022.
- [40] A. R. Alt and C. R. Bolognesi, "(InP) HEMT small-signal equivalent-circuit extraction as a function of temperature," *IEEE Trans. Microw. Theory Techn.*, vol. 63, no. 9, pp. 2751–2755, Sep. 2015.
- [41] D. K. Schroder, Semiconductor Material and Device Characterization, 3rd ed., Hoboken, NJ, USA: Wiley, 2015.
- [42] M. W. Pospieszalski, "Extremely low-noise amplification with cryogenic FETs and HFETs: 1970-2004," *IEEE Microw. Mag.*, vol. 6, no. 3, pp. 62–75, Sep. 2005.
- [43] J. Schleeh et al., "Phonon black-body radiation limit for heat dissipation in electronics," *Nature Mater.*, vol. 14, no. 2, pp. 187–192, Feb. 2015.
- [44] A. Y. Choi, I. Esho, B. Gabritchidze, J. Kooi, and A. J. Minnich, "Characterization of self-heating in cryogenic high electron mobility transistors using Schottky thermometry," *J. Appl. Phys.*, vol. 130, no. 15, Oct. 2021, Art. no. 155107.
- [45] A. J. Ardizzi et al., "Self-heating of cryogenic high electron-mobility transistor amplifiers and the limits of microwave noise performance," J. Appl. Phys., vol. 132, no. 8, Aug. 2022, Art. no. 084501.
- [46] G. D. J. Smit, A. J. Scholten, R. M. T. Pijper, R. van Langevelde, L. F. Tiemeijer, and D. B. M. Klaassen, "Experimental demonstration and modeling of excess RF noise in sub-100-nm CMOS technologies," *IEEE Electron Device Lett.*, vol. 31, no. 8, pp. 884–886, Aug. 2010.
- [47] C.-H. Chen and M. J. Deen, "Channel noise modeling of deep sub-micron MOSFETs," *IEEE Trans. Electron Devices*, vol. 49, no. 8, pp. 1484–1487, Aug. 2002.
- [48] V. M. Mahajan, R. P. Jindal, H. Shichijo, S. Martin, F.-C. Hou, and D. Trombley, "Numerical investigation of excess RF channel noise in sub-100 nm MOSFETs," in *Proc. 2nd Int. Workshop Electron Devices Semiconductor Technol.*, Jun. 2009, pp. 1–4.

- [49] G. D. J. Smit, A. J. Scholten, R. M. T. Pijper, L. F. Tiemeijer, R. van der Toorn, and D. B. M. Klaassen, "RF-noise modeling in advanced CMOS technologies," *IEEE Trans. Electron Devices*, vol. 61, no. 2, pp. 245–254, Feb. 2014.
- [50] A. J. Scholten, G. D. J. Smit, R. M. T. Pijper, and L. F. Tiemeijer, "Benchmark tests for MOSFET thermal noise models," in *Noise Nanoscale Semiconductor Devices*, T. Grasser, Ed., Cham, Switzerland: Springer, 2020, pp. 687–710.
- [51] A. H. Akgiray, "New technologies driving decade-bandwidth radio astronomy: Quad-ridged flared horn and compound-semiconductor LNAs," Ph.D. dissertation, Dept. Eng. Sci., Cal. Inst. Tech., Pasadena, CA, USA, 2013.
- [52] D. C. Ruiz, T. Saranovac, D. Han, O. Ostinelli, and C. R. Bolognesi, "Impact ionization control in 50 nm low-noise high-speed InP HEMTs with InAs channel insets," in *IEDM Tech. Dig.*, Dec. 2019, pp. 9.3.1–9.3.4.
- [53] B. G. Vasallo, J. Mateos, D. Pardo, and T. González, "Kink-effect related noise in short-channel InAlAs/InGaAs high electron mobility transistors," *J. Appl. Phys.*, vol. 95, no. 12, pp. 8271–8274, Jun. 2004.
- [54] X. Chen, H. Elgabra, C.-H. Chen, J. Baugh, and L. Wei, "Estimation of MOSFET channel noise and noise performance of CMOS LNAs at cryogenic temperatures," in *Proc. IEEE Int. Symp. Circuits Syst.* (ISCAS), May 2021, pp. 1–5.
- [55] S. K. Kim, A. van der Ziel, and S. T. Liu, "Hot electron noise effects in buried channel MOSFETs," *Solid-State Electron.*, vol. 24, no. 5, pp. 425–428, May 1981.
- [56] B. Gabritchidze, K. Cleary, A. Readhead, and A. J. Minnich, "Investigation of drain noise in InP pHEMTs using cryogenic on-wafer characterization," in *IEEE MTT-S Int. Microw. Symp. Dig.*, Jun. 2023, pp. 16–19.
- [57] M. R. Murti et al., "Temperature-dependent small-signal and noise parameter measurements and modeling on InP HEMTs," *IEEE Trans. Microw. Theory Techn.*, vol. 48, no. 12, pp. 2579–2587, Feb 2000
- [58] A. J. Scholten et al., "Accurate thermal noise model for deep-submicron CMOS," in *IEDM Tech. Dig.*, Dec. 1999, pp. 155–158.
- [59] C. Jungemann et al., "Hydrodynamic modeling of RF noise in CMOS devices," in *IEDM Tech. Dig.*, Jun. 2003, p. 36.
- [60] S. N. Ong et al., "Impact of velocity saturation and hot carrier effects on channel thermal noise model of deep sub-micron MOSFETs," *Solid-State Electron.*, vol. 72, pp. 8–11, Jun. 2012.
- [61] C. Jungemann and B. Meinerzhagen, "Do hot electrons cause excess noise?" Solid-State Electron., vol. 50, no. 4, pp. 674–679, Apr. 2006.
- [62] S. Y. Chou and D. A. Antoniadis, "Relationship between measured and intrinsic transconductances of FET's," *IEEE Trans. Electron Devices*, vol. ED-34, no. 2, pp. 448–450, Feb. 1987.
- [63] J. Shah, "Hot carriers in quasi-2-D polar semiconductors," IEEE J. Quantum Electron., vol. QE-22, no. 9, pp. 1728–1743, Sep. 1986.
- [64] H. Rodilla, J. Schleeh, P.-Å. Nilsson, N. Wadefalk, J. Mateos, and J. Grahn, "Cryogenic performance of low-noise InP HEMTs: A Monte Carlo study," *IEEE Trans. Electron Devices*, vol. 60, no. 5, pp. 1625–1631, May 2013.
- [65] M. V. Fischetti, "Monte Carlo simulation of transport in technologically significant semiconductors of the diamond and zinc-blende structures. I. Homogeneous transport," *IEEE Trans. Electron Devices*, vol. 38, no. 3, pp. 634–649, Mar. 1991.
- [66] J. Huang, T. Y. Chang, and B. Lalevic, "Measurement of the conductionband discontinuity in pseudomorphic In_xGa_{1-x}As/In_{0.52}Al_{0.48}As heterostructures," *Appl. Phys. Lett.*, vol. 60, no. 6, pp. 733–735, 1992.
- [67] S. Bahl, W. Azzam, and J. del Alamo, "Strained-insulator In_xAl_{1-x}As/n+-In_{0.53}Ga_{0.47}As heterostructure field-effect transistors," *IEEE Trans. Electron Devices*, vol. 38, no. 9, pp. 1986–1992, Ian 1991
- [68] G. Gonzalez, Microwave Transistor Amplifiers: Analysis and Design. Upper Saddle River, NJ, USA: Prentice-Hall, 1984.
- [69] G. Hallinan et al., "The DSA-2000—A radio survey camera," 2019, arXiv:1907.07648.